JOURNAL OF CATALYSIS **118**, 192–202 (1989)

Pt–Ir/Al_2O_3 Catalysts—The Effect of Pt–Ir Interaction on Ir Agglomeration and Catalytic Performance

Y.-J. HUANG,[1] S. C. FUNG, W. E. GATES, AND G. B. MCVICKER

Exxon Research and Engineering Company, Corporate Research Laboratories, Clinton Township, Rt. 22 East, Annandale, New Jersey 08801

Received October 3, 1988; revised March 10, 1989

Interaction between Pt and Ir has been found to occur on freshly impregnated Pt–Ir/Al_2O_3 subjected only to drying at 393 K. Iridium in the freshly prepared bimetallic precursor material retains the same reduction behavior as monometallic Ir. Iridium promotes the reduction of Pt in the bimetallic precursor material. This promotion results in a 20 K lower temperature-programmed reduction peak temperature than that observed for monometallic Pt. The incorporation of Pt into Ir clusters retards the oxidative agglomeration of Ir. Reduction followed by calcination causes a higher degree of Ir oxidative agglomeration than direct calcination at the same temperature. The incorporation of Pt into Ir clusters decreases the cracking activity of the Ir component as well as the coking tendency of the Pt component, and therefore enhances benzene selectivity. The catalytic performance of a Pt–Ir catalyst approaches that of a Pt-only catalyst as the degree of Ir agglomeration increases. The cracking of *n*-hexane molecules takes place more frequently at the terminal carbon atom position as the degree of Ir agglomeration increases.

INTRODUCTION

Supported Pt and Ir catalysts have been the subject of much research. Numerous researchers (*1–6*) have used techniques such as EXAFS, selective gas chemisorption, X-ray diffraction, Mössbauer spectroscopy, and chemical probe reactions to detect the presence of Pt–Ir interaction. Interaction between Pt and Ir has been assumed to occur during catalyst reduction. Recent laser Raman studies of Pt–Ir/Al_2O_3 catalysts by Chan *et al.* (*7*) have indicated, however, that interaction between the two metals may in fact take place upon drying the freshly impregnated materials.

Sinfelt (*8*) has demonstrated that incorporation of Pt into Ir clusters retards the oxidative agglomeration of iridium at high temperatures. The agglomeration process results in the segregation of Ir from the Pt–Ir bimetallic clusters. These separated iridium phases can be detected by X-ray diffraction, TEM, and EXAFS measurements. Recently, Huang and co-workers (*9, 10*) have demonstrated the use of temperature-programmed reduction (TPR) techniques to infer the structure and component separation of Pt–Ir surface species.

Phase separation often alters the catalytic properties of bimetallic catalysts. McVicker and Ziemiak (*2*) have shown that an inverse relationship exists between either the rate of dehydrocyclization of *n*-heptane or naphtha reforming activity and the degree of iridium agglomeration in a Pt–Ir bimetallic catalyst.

The purpose of this study was to further explore the effect of Pt–Ir interaction on Ir agglomeration and the performance of the Pt–Ir/Al_2O_3 catalysts subjected to different treatment conditions. Freshly impregnated and 393 K dried materials were examined to assess the interaction between Pt and Ir in their precursor stages. Subsequently, two different treatments were employed on these precursor materials: (i) calcining the

---

[1] To whom correspondence should be addressed at Exxon Chemical Co. P.O. Box 4900, Baytown, TX 77522-4900.

0021-9517/89 $3.00

catalyst precursors in air or (ii) reducing the catalyst precursors in H_2, followed by air calcination. The evolution and composition of metal species as well as the degree of Ir agglomeration after the above treatments were characterized by TPR. The effect of catalyst treatment conditions on *n*-hexane conversion was also determined.

EXPERIMENTAL

Catalysts

The monometallic and bimetallic catalysts used in this study were prepared on γ-Al_2O_3 supplied by Ketjen. Prior to use, the γ-Al_2O_3 extrudates ($\frac{1}{16}$ in.) were calcined at 773 K for 6 h and ground to a particle size range of 40 to 80 mesh. The surface area of the support was about 200 m^2/g. Chloroplatinic and chloroiridic acids were used to prepare the electrolyte solutions, and their concentrations were adjusted to prepare 2.31 and 1.45 wt% of Pt and Ir, respectively. The chloroplatinic acid solution was prepared by dissolving chloroplatinic acid crystals (supplied by Engelhard) in doubly distilled water. The chloroiridic acid solution containing 10.024 wt% Ir and 14.02 wt% Cl was supplied by Johnson Matthey. Twenty grams of 40/80 mesh γ-Al_2O_3 particles were immersed in 50 cm^3 of the impregnation solution (wet impregnation), and the resulted slurry was shaken constantly for 24 h. The slurry was evaporated to dryness at room temperature over a 24-h period. The samples were further dried in air at 393 K for 16 h.

The above dry precursor materials were subjected to two different treatments. A portion of the dry precursor materials was calcined in a muffle furnace under flowing air. The materials were brought to 393 K at a heating rate of 5 K/min and maintained at this temperature for 1 h. The temperature was then increased to either 593 or 693 K at a heating rate of 5 K/min and held at the target temperature for 4 h. A second portion of the dry precursor materials was reduced in a tubular reactor under 20% H_2 in He (1000 cm^3/min). The reduction temperature was increased to 723 K (5 K/min) and maintained at this temperature for 3 h. The reduced catalysts were allowed to cool to room temperature under He (1000 cm^3/min). The reduced catalysts were subsequently calcined in a muffle furnace with the same procedures described above.

Temperature-Programmed Reduction

Apparatus. The apparatus used in this study consisted of three major sections: gas purification/control system, reactor, and detector assembly. Reactor temperature, controlled by an Omega microprocessor temperature programmer, was measured at the center of the bed. Hydrogen consumption during the TPR experiments was monitored by an IBM PC-XT interfaced to a Fisher Model 1200 gas partitioner with a built-in thermal conductivity cell. A more detailed description of the TPR apparatus can be found in the literature (*9, 10*).

Procedures. One-hundred-milligram samples were dehydrated under Ar (100 cm^3/min). The precursor materials were dehydrated at 393 K to avoid decomposition of the precursor complexes. The calcined or reduced/calcined samples were dehydrated at 773 K (5 K/min) for 1 h. The samples were then allowed to cool to room temperature.

The Ar stream was adjusted to 40 cm^3/min and directed to the TCD. After the TCD was stabilized, several pulses of 8.5% H_2/Ar were injected into the reactor via an internal sampling loop with a volume of 0.55 cm^3 per pulse. The injection of H_2/Ar was repeated until H_2 breakthrough occurred. The amount of H_2 consumed at this point was attributed to reduction of the samples at room temperature.

The Ar stream was then switched to 8.5% H_2/Ar at a flow rate of 57 cm^3/min. After the TCD was stabilized, several pulses of Ar (0.55 cm^3/pulse) were then injected into the reactor to calibrate the time lag of the response from the TCD. After the TCD was calibrated (typically a 3 K lag was found), the temperature of the reactor was raised to 823 K at a heating rate of 20 K/min and held at 823 K for 30 min. The H_2 consumption data and temperature of the catalyst bed were recorded as a function of time by an IBM PC-XT.

X-Ray Diffraction Analysis

A Phillips Electronics X-ray diffractometer (XRG-3000) with nickel-filtered Cu*K* radiation was used for X-ray diffraction studies of the samples. The relative amounts of IrO_2 and Ir agglomeration between samples were calculated from the area ratios of their $IrO_2(110)$ and Ir(111) lines, respectively. We preferred using X-ray diffraction measurements rather than hydrogen chemisorption in comparing iridium agglomeration among samples, since X-ray directly measures the amount of Ir agglomerates and hydrogen chemisorption gives more emphasis to the highly dispersed phase.

n-Hexane Conversion

Experiments were carried out in a single-pass fixed-bed stainless steel $\frac{1}{4}$-in.-o.d. reactor. A 0.2-g sample was used in each experiment. The sample was mixed with 3.8-g quartz particles in a size range between 40 and 80 mesh. The catalysts were dried at 423 K under N_2 (300 cm^3/min). Hydrogen (300 cm^3/min at 343 kPa above atmospheric pressure) was introduced into the reactor at 423 K, and the catalyst temperature was increased to 673 K (3.5 K/min), where it was maintained for $\frac{1}{2}$ h. The feed was introduced into the reactor at this temperature. The feed contained 565 cm^3/min of H_2 and 0.5 cm^3/min of liquid *n*-hexane. A flow of 29 cm^3/min of N_2 was introduced into the feed as a tracer. The pressure was 720 kPag above atmospheric pressure and the *n*-C_6 liquid feed space velocity was normally 100 WHSV throughout the experiments. The reaction was carried out at 673 K for 12 h to tune down the cracking activity before the reaction temperature was raised to 773 K. The product distributions were analyzed by on-line GC at 1-hr intervals, and sampling was continued for 12 h.

RESULTS AND DISCUSSION

TPR Experiments

393 K dried precursor materials. To explore whether interactions between the Pt and the Ir occur at their precursor stage, TPR experiments were performed on the samples dried at 393 K. Figure 1 shows the TPR spectra of dried 2.31% Pt, 1.45% Ir, and 2.31% Pt/1.45% Ir on Al_2O_3. The TPR peak temperature of the Pt sample occurred at 478 K, while the Ir sample exhibited a maximum at 383 K and a shoulder at 458 K. The bimetallic sample displayed peak temperatures at 383 and 458 K. Thus, the TPR spectrum of the bimetallic catalyst is not the superposition of the spectra of the individual components. The reduction behaviors of Ir in the bimetallic and monometallic cases are similar. Platinum in the bimetallic case exhibits a shift in its peak temperature to a value 20 K lower than that for the monometallic Pt sample. Thus, Ir appears to promote the reduction of Pt.

Directly calcined samples. Figure 2 shows the TPR spectra of Pt, Ir, and Pt–Ir/Al_2O_3 catalysts directly calcined at 693 K. The Pt catalyst exhibits a pair of peaks at 373 and 438 K, whereas Ir displayed a sharp peak maximum at 488 K and a broad peak at 523 K. The Pt–Ir bimetallic catalyst demonstrated three peak maxima at 378, 433, and 478 K, respectively. Thus, the TPR spectrum of the bimetallic catalyst is not the superposition of the individual components. Complete reduction of the bimetallic catalyst occurs at lower temperatures than that of the individual monometallic catalysts. The most significant difference between the bimetallic catalyst and its individual components is the increase in the area under the peak at 433 K.

Additionally, it is interesting to note that when the monometallic Ir (Fig. 3) was first reduced and then calcined it showed sub-

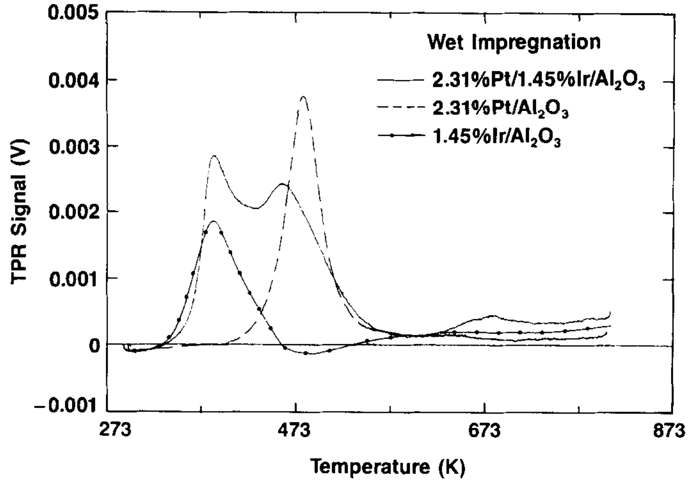

FIG. 1. TPR spectra of 2.31% Pt, 1.45% Ir, and 2.31% Pt/1.45% Ir on Al_2O_3 dried at 393 K.

stantially less oxidized iridium then the directly calcined sample (Fig. 2). This suggests that the reduced sample contained some large Ir metal agglomerates due to high metal loading and method of preparation. We have demonstrated by X-ray diffraction that Ir metal particles greater than 10 nm did not show an IrO_2 diffraction peak after high-temperature air calcination. But the diffraction spectrum still showed metallic Ir, although its intensity was reduced. It appears that oxidation of the entire Ir metal agglomerate is prevented by the surface oxide layers. Because of the presence of large Ir metal agglomerates, the reduced and calcined sample showed substantially less oxidized iridium in its TPR spectrum, whereas all the iridium in the directly calcined sample started out at its 4+ state and stayed at this state through out the calcination step.

In order to identify the surface species responsible for the peaks observed in the TPR experiments, several additional experiments were performed. The impregnated and 393 K dried Pt and Ir monometallic

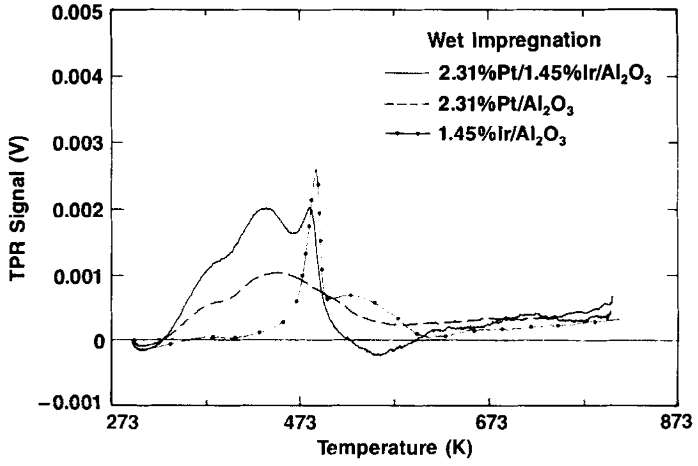

FIG. 2. TPR spectra of Pt, Ir, and Pt–Ir/Al_2O_3 catalysts directly calcined at 693 K.

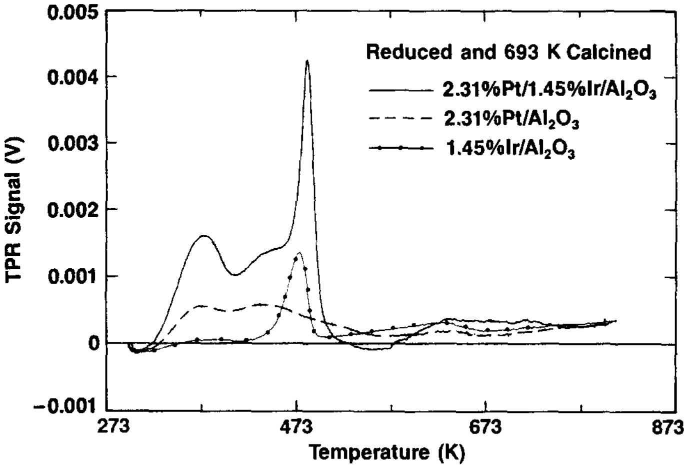

FIG. 3. TPR spectra of Pt, Ir, and Pt–Ir/Al_2O_3 catalysts directly reduced at 723 K and then calcined at 693 K.

catalysts were reduced first at 723 K and then calcined at 693 K. The TPR spectra for these two catalysts are shown in Fig. 3. The Pt catalyst displays two peaks at 373 and 438 K, while the Ir catalyst exhibits a single peak at 478 K. The peak positions of the bimetallic catalysts coincide with the peaks shown by the monometallic catalysts. It is well known that highly dispersed Ir metal clusters agglomerate at a temperature higher than 693 K (*3*, *4*, *11*), and indeed with an Ir sample that had been heated at 773 K for 16 h (to deliberately sinter iridium to large IrO_2 particles), TPR showed a peak at 483 K. Therefore, the peak observed at 478 K for the reduced and calcined Ir sample is likely due to agglomerated IrO_2. This indicates that interactions between Pt and Ir took place in the catalyst precursor state prior to hydrogen reduction. These interactions stabilized iridium and minimized its agglomeration to large IrO_2 particles when the bimetallic sample was directly calcined at high temperatures, as indicated by Fig. 2. Additionally, these interactions promoted the decomposition of Pt and Ir chloride complexes to oxygen-rich species leading to the formation of highly dispersed mixed Pt–Ir oxides as is indicated by the lack of broad peaks at temperatures higher than 493 K (they appeared in the cases of monometallic catalysts) *and* the increase in the peak area at 433 K in the TPR spectrum of the Pt–Ir/Al_2O_3 catalyst, as shown in Fig. 2. It is proposed that the low-temperature peak may be due to Pt^{2+} species and the high-temperature peak may be due to Pt^{4+} and Ir^{4+} mixed species. Wagstaff and Prins (*12*) have performed similar experiments by using a highly dispersed 0.75 wt% Pt catalyst. They showed that the Pt^{2+} species reduced at about 373 K and the reduction of Pt^{4+} species started at about 423 K.

Figure 4 shows the TPR of the Pt–Ir bimetallic catalyst subjected to 593 and 693 K calcinations. The catalyst calcined at 593 K had a major peak at 433 K and a small shoulder at 378 K. It is apparent that the 593 K calcination induced essentially no agglomerated IrO_2 phase. No IrO_2 phase was detected by X-ray measurements and therefore no large IrO_2 particles were produced. Furthermore, it is interesting to note that in the case of H_2PtCl_6/Al_2O_3 catalyst, calcination temperatures of 593 and 693 K are not high enough to completely decompose the Pt chloride complexes. This conclusion is based on the retention of the yellow color (color of the impregnated and

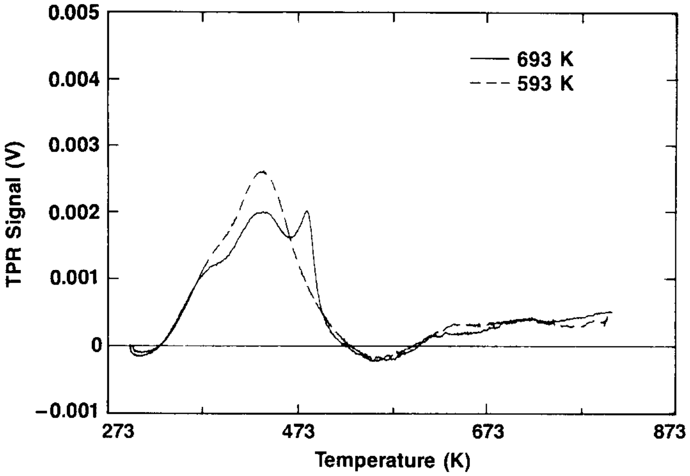

FIG. 4. TPR spectra of the Pt–Ir/Al_2O_3 catalyst subjected to 593 and 693 K calcination.

393 K dried catalyst) and a broad TPR peak extended beyond 493 K (Fig. 2). This is in agreement with the reported TGA studies on the bulk H_2PtCl_6 (*13*). In the case of bimetallic catalyst the presence of highly dispersed IrO_2 appears to promote the decomposition of both the platinum and the iridium oxychloride complexes to mixed metal oxides as has been discussed earlier. Therefore, it is reasonable to conclude that the peaks observed at about 373, 433, and 483 K (with an accuracy of 10 K) are due to highly dispersed Pt^{2+}, bimetallic Pt–Ir oxygen-rich complexes, and agglomerated IrO_2, respectively. The existence of the agglomerated IrO_2 particles can be easily identified by their sharp reduction peak at about 483 K in the TPR spectrum.

Directly reduced and subsequently calcined samples. Pt–Ir bimetallic catalysts were directly reduced at 723 K and calcined at either 593 or 693 K to assess the extent of Ir agglomeration resulting from the oxidative segregation of the bimatallic clusters. Figure 5 shows the TPR spectrum of the directly reduced Pt–Ir bimetallic catalysts

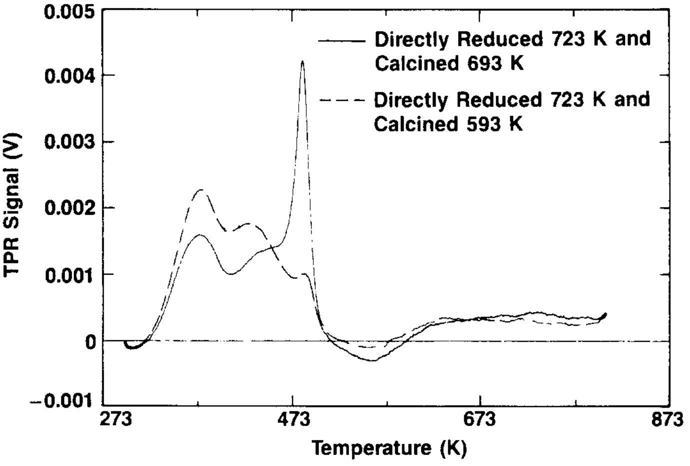

FIG. 5. TPR spectra of Pt–Ir/Al_2O_3 catalysts directly reduced at 723 K and then calcined at either 593 or 693 K.

subjected to 593 and 693 K calcination, respectively. As shown in Fig. 5, the above treatments result in peaks at 378, 433, and 478 K. X-ray diffraction detected no agglomerated Ir phase in the directly reduced sample. The subsequent 593 K calcination of the prereduced sample thus resulted in a small degree of phase separation and IrO_2 agglomeration, as indicated by the appearance of an agglomerated IrO_2 phase by TPR. The extent of Ir agglomeration increases dramatically when the prereduced catalyst is calcined at 693 K. It is apparent from the TPR spectra that the fraction of highly dispersed Pt–Ir clusters (peak at 433 K) decreases and agglomerated IrO_2 (peak at 483 K) increases with increasing calcination temperature. The loss of the Pt^{2+} species with increasing calcination temperature is in agreement with the results reported by Huizinga *et al.* (*14*) indicating that more Pt^{2+} species are being oxidized to Pt^{4+}. The observed decrease in the peak area at 433 K after 693 K calcination is due to a decrease in the contribution from highly dispersed Ir^{4+}, because of an increase in IrO_2 agglomeration.

Differences in the TPR spectra between directly calcined samples (Fig. 4) and the directly reduced and subsequently calcined samples (Fig. 5) are apparent. The former samples are less agglomerated than the latter ones. These inferences were confirmed by X-ray diffraction. For the 693 K calcination temperature, X-ray diffraction results demonstrated that the IrO_2 agglomeration in the directly calcined sample was about seven times less than the reduced and calcined sample. After 723 K hydrogen reduction both platinum and iridium are in their metallic states forming highly dispersed bimetallic clusters. Although the presence of Pt in the bimetallic clusters imparts some stability to iridium against oxidative agglomeration, the large difference in their reactivities toward oxygen results in the formation of iridium oxide at a temperature where platinum may still remain in the metallic state leading to the separation of the IrO_2 phase and its subsequent agglomeration. In the case of directly calcined samples both platinum and iridium start in the 4+ oxidation state. Under oxygen at high-temperatures, interaction between Pt and Ir through the formation of mixed oxychloride and oxide complexes stabilizes iridium in a highly dispersed state on the one hand and promotes the decomposition of platinum and iridium chlorides on the other.

n-Hexane Conversion

Both the calcined and the uncalcined catalysts were used in this study. The directly reduced and subsequently calcined $Pt–Ir/Al_2O_3$ catalyst, which has a high degree of Ir agglomeration, was used in the *n*-hexane conversion study to emphasize the effect of Ir agglomeration on reaction kinetics. Please note that the conditions for high conversion level were chosen to simulate the conversion levels used in commercial reforming operations.

n-C_6 conversion is defined as the ratio of moles of *n*-C_6 that disappeared to moles of *n*-C_6 in the feed. The selectivity to a particular product is defined as the ratio of moles of *n*-C_6 converted to that product to total moles of *n*-C_6 converted.

Total conversion. Figure 6 shows the total conversion of *n*-C_6 of as a function of time. Uncalcined Ir had a conversion of 10% higher than calcined Ir. Both uncalcined and calcined Pt–Ir started at a lower conversion level, but steadily increased with time. At the end of 12 h, the uncalcined Pt–Ir reached the same conversion level as the uncalcined Ir. Although the difference is small, uncalcined Pt–Ir maintained a higher conversion level than the calcined Pt–Ir. The reduced and calcined Pt–Ir deviated dramatically. It started at a low activity, but activity increased with time after 4 h into the run. The similarity in the time-dependent activity patterns between the reduced and calcined Pt–Ir and the rest of the Pt–Ir catalysts indicates that the highly agglomerated Pt–Ir still pos-

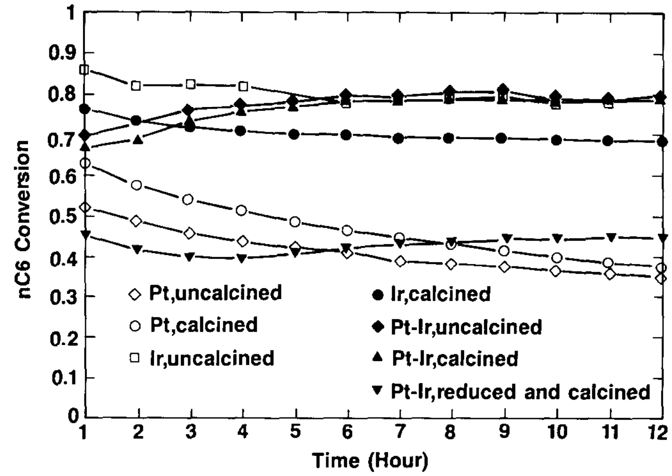

FIG. 6. Total conversion of *n*-hexane as a function of time.

sesses the activity maintenance of a bimetallic catalyst. However, due to its severe Ir agglomeration, its activity was maintained at a lowered level. The uncalcined and calcined Pt samples had a lower activity than the other catalysts, and their activities decreased with time. This decrease in the activity as a function of time strongly suggests the gradual poisoning of the catalysts by coke.

Selectivity to methane. Figure 7 shows the selectivity to methane as a function of the reaction time. Iridium catalysts maintained their methane selectivities of about 80%. All the other catalysts exhibit methane selectivities of less than 13%.

It is apparent from the methane selectivity that the incorporation of Pt into Ir alters the cracking activity of Ir. Platinum enrichment on the surface of the bimetallic clusters leading to reduction of Ir ensemble size may be the main reason for the bimetallic catalysts showing a lower cracking activity than that of the monometallic iridium catalysts. It is surprising that the agglomerated monometallic iridium (calcined Ir catalyst) showed a much higher (by a factor of more than 1.6) n-C_6 conversion activity than the

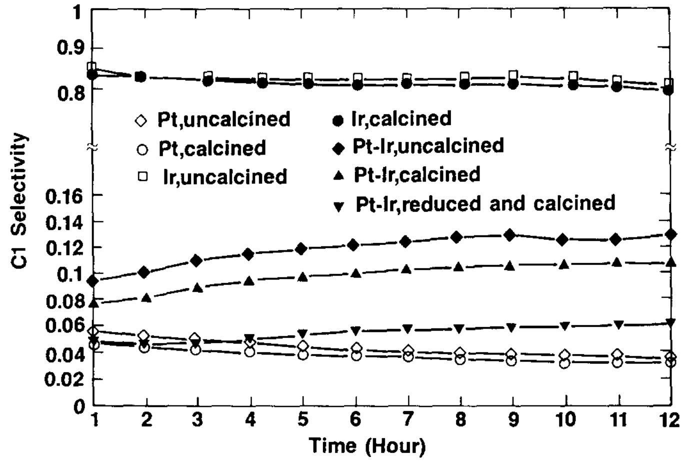

FIG. 7. Methane selectivity as a function of time.

reduced and calcined bimetallic catalyst where platinum in the latter was still highly dispersed. Furthermore, the activity of the former was reflected mainly in methane production (methane selectivity >80%). It appears that the reduced cracking activity exhibited by the agglomerated iridium particles in the reduced and calcined bimetallic catalyst may be due to platinum enrichment in the surface of agglomerated Ir particles. The severely agglomerated Pt–Ir catalyst behaves like the monometallic Pt catalysts in both n-C_6 conversion and methane selectivity.

Selectivity to benzene. Figure 8 shows benzene selectivity as a function of time. The most striking effect is the high benzene selectivity of the bimetallic catalysts. One may invoke a synergistic effect to account for this observation. However, we favor an alternative explanation based on their different responses to deactivation by coke. Both calcined and uncalcined Ir catalysts have benzene selectivities of about 3.5%. Since iridium is known to be a very efficient cracking catalyst, a low benzene selectivity is expected. The benzene selectivity of the Pt catalysts decreased dramatically at the beginning of the experiments and then leveled off. The bimetallic catalysts are superior to the monometallic catalysts in this respect. The selectivities to benzene for the bimetallic catalysts were maintained at a higher level than the monometallic catalysts since coke deactivation of the Pt component was greatly diminished due to the high hydrogenolysis activity of iridium causing the destruction of coke precursors. Furthermore, the Pt component in the Pt–Ir cluster alters the Ir cracking ability. The combination of the two factors results in the maintenance of high selectivity to benzene. The reduced and calcined Pt–Ir has a lower selectivity to benzene than the rest of the Pt–Ir samples. This indicates that the high degree of Ir agglomeration lowers the concentration of iridium in the Pt–Ir clusters and this results in a decrease in the Ir hydrogenolysis activity and thus a decrease in the rate of destruction of coke precursors on the clusters.

Terminal cracking index. Terminal cracking index (TCI) is defined as the ratio of the total C_5 formation to total C_4 formation. It describes the position at which cracking takes place. The higher the value, the more frequent cracking occurs at the end of the n-C_6 molecules. However, due to the definition of the TCI this statement is valid when there is little subsequent cracking of the C_5 and C_4 molecules. When there is extensive secondary cracking, C_5 and C_4 molecules produced from the primary cracking of n-C_6 are destroyed to

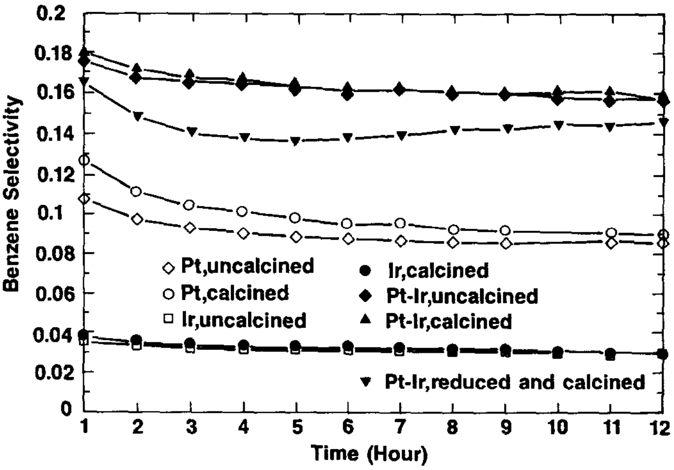

FIG. 8. Benzene selectivity as a function of time.

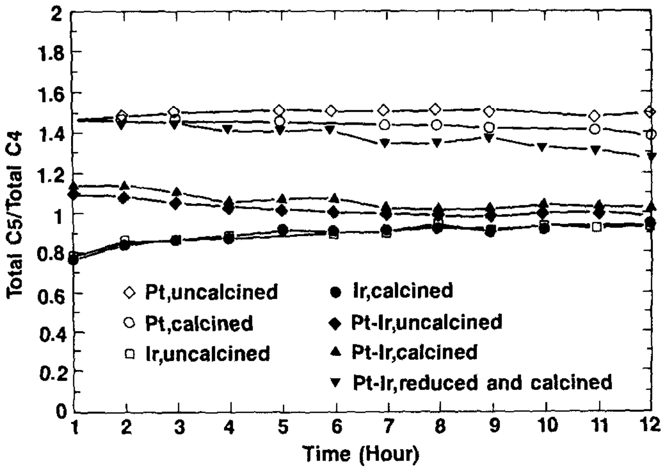

FIG. 9. Terminal cracking index as a function of time.

about the same extent. But new C_4 molecules are generated from the cracking of C_5 molecules when the latter crack at the terminal C–C bonds. Therefore, with extensive secondary cracking the TCI tends to shift to a lower value. This is the situation encountered by the uncalcined and calcined iridium catalysts. There is no physical meaning in their TCI since extensive secondary cracking occurred as was indicated by >80% methane selectivity. The addition of platinum to iridium reduced methane selectivity to below 13% and thus greatly lowered its secondary cracking activity. Figure 9 shows the terminal cracking index of different catalysts as a function of reaction time. It was found that Pt catalysts maintained a higher tendency to crack n-C_6 molecules at the end as was indicated by TCI > 1.4. When Pt and Ir form bimetallic clusters, the cracking position appears to be more random as was indicated by a lowering of the TCI to about 1. The TCI of the bimetallic catalysts increased to the level of platinum only when most of the iridium was agglomerated to large particles as in the case of the reduced and calcined sample.

SUMMARY

(i) On the bimetallic Pt–Ir precursor materials which are dried at 393 K, the reduction of Ir occurs at a lower temperature than that of Pt. Iridium in the freshly prepared bimetallic precursor materials retains the same reduction behavior as monometallic Ir. Iridium promotes the reduction of Pt in the bimetallic precursor material. This promotion results in a 20 K lower TPR peak temperature than that observed for monometallic Pt. The TPR spectrum of the bimetallic precursor material is not equal to the superposition of the TPR spectra of its individual components.

(ii) The TPR peaks observed at about 373, 433, and 483 K are due to the highly dispersed Pt^{2+}, the highly dispersed Pt^{4+} and/or bimetallic Pt–Ir oxygen-rich complexes, and the agglomerated IrO_2, respectively. The existence of the agglomerated IrO_2 particles can be easily identified by their sharp reduction peak at about 483 K in the TPR spectrum.

(iii) The incorporation of Pt into Ir clusters retards the oxidative agglomeration of Ir. When the bimetallic catalysts are calcined at 593 K, the majority of the surface species are bimetallic Pt–Ir oxychloride complexes. No significant IrO_2 agglomeration is observed. When the catalysts are calcined at 693 K, Pt^{2+}, bimetallic Pt–Ir oxygen-rich chloride complexes, and IrO_2 are observed by TPR.

(iv) The bimetallic precursor materials

subjected to reduction followed by calcination have a higher degree of Ir agglomeration than those receiving direct high-temperature air calcination. It is proposed that the interaction between Pt and Ir through the formation of mixed oxygen–chloride complexes stabilizes iridium in a highly dispersed phase and promotes platinum to form oxygen-rich complexes.

(v) The catalytic performance of the highly agglomerated Pt–Ir catalyst is similar to that of Pt catalysts. Incorporation of Pt into Ir clusters decreases the cracking activity of the Ir and enhances the benzene selectivity. The cracking of *n*-hexane molecules takes place more frequently at the terminal carbon position as the degree of Ir agglomeration increases.

(vi) The benzene selectivity for the bimetallic catalysts at 773 K was maintained at a level substantially higher than that of their monometallic catalysts. This finding was attributed to (i) high hydrogenolysis activity of iridium in destroying coke precursors *and* (ii) alteration of Ir cracking activity by Pt components in the Pt–Ir clusters.

The effect of preparation procedures in bimetallic Pt–Ir catalysts on metal cluster composition, phase separation, and Ir agglomeration was demonstrated by TPR. The results obtained by TPR were also reflected in changes in *n*-hexane aromatization activity and selectivity.

ACKNOWLEDGMENTS

The authors acknowledge Professor Jan-fan Hu for her assistance in TPR experiments and Dr. J. H. Sinfelt for helpful discussion. We also thank Professor J. A. Schwarz for assessing the TPR apparatus at Syracuse University.

REFERENCES

1. Sinfelt, J. H., Via, G. H., and Lytle, F. W., *J. Chem. Phys.* **76,** 2779 (1982).
2. McVicker, G. B., and Ziemiak, J. J., *Appl. Catal.* **14,** 229 (1985).
3. Garten R. L., and Sinfelt, J. H., *J. Catal.* **62,** 127 (1980).
4. Sinfelt J. H., and Via, G. H., *J. Catal.* **56,** 1 (1979).
5. Pearson, W. B., "A Handbook of Lattice Spacings and Structures of Metals and Alloys," p. 704. Pergamon, New York, 1964.
6. Graham, A. G., and Wanke, S. E., *J. Catal.* **68,** 1 (1981).
7. Chan, S. C., Fung, S. C., and Sinfelt, J. H., *J. Catal.* **113,** 164 (1988).
8. Sinfelt, J. H., "Bimetallic Catalysts—Discoveries, Concepts, and Applications," p. 93. Wiley, New York, 1983.
9. Huang, Y.-J., Xue, J., and Schwarz, J. A., *J. Catal.* **111,** 59 (1988).
10. Xue, J., Huang, Y.-J., and Schwarz, J. A., *Appl. Catal.*, in press.
11. Sinfelt, J. H., U.S. Patent 3,953,368 (1976).
12. Wagstaff N., and Prins, R., *J. Catal.* **59,** 434 (1979).
13. Schweizer, A. E., and Kerr, G. T., *Inorg. Chem.* **17**(8), 2326 (1978).
14. Huizinga, T., van Grondelle, J., and Prins, R., *Appl. Catal.* **10,** 199 (1984).